

ANL-6373
Physics
(TID-4500, 16th Ed.)
AEC Research and
Development Report

ARGONNE NATIONAL LABORATORY
9700 South Cass Avenue
Argonne, Illinois

THEORETICAL REACTION CROSS SECTIONS
FOR ALPHA PARTICLES WITH AN
OPTICAL MODEL

by

J. R. Huizenga* and G. J. Igo**

*Chemistry Division

**Lawrence Radiation Laboratory, Berkeley, California

May 1961

Operated by The University of Chicago
under
Contract W-31-109-eng-38

DISCLAIMER

This report was prepared as an account of work sponsored by an agency of the United States Government. Neither the United States Government nor any agency Thereof, nor any of their employees, makes any warranty, express or implied, or assumes any legal liability or responsibility for the accuracy, completeness, or usefulness of any information, apparatus, product, or process disclosed, or represents that its use would not infringe privately owned rights. Reference herein to any specific commercial product, process, or service by trade name, trademark, manufacturer, or otherwise does not necessarily constitute or imply its endorsement, recommendation, or favoring by the United States Government or any agency thereof. The views and opinions of authors expressed herein do not necessarily state or reflect those of the United States Government or any agency thereof.

DISCLAIMER

Portions of this document may be illegible in electronic image products. Images are produced from the best available original document.

TABLE OF CONTENTS

	<u>Page</u>
ABSTRACT	3
I. INTRODUCTION.	3
II. RESULTS AND DISCUSSION	4
A. Simplified Calculation of Reaction Cross Sections with a Parabolic Approximation of Optical Model Real Potential ..	19
B. Comparison of Reaction Cross Sections from Various Models	19
C. Optical-model Cross-section Dependence on Nuclear Potential	24
D. Program Checks	27
III. ACKNOWLEDGMENTS	27
REFERENCES	28

THEORETICAL REACTION CROSS SECTIONS
FOR ALPHA PARTICLES WITH AN
OPTICAL MODEL

by

J. R. Huizenga and G. J. Igo

ABSTRACT

The transmission coefficients T_ℓ and total reaction cross sections σ_R for alpha particles in the energy range 0-46 Mev interacting with twenty target nuclei with atomic numbers ranging from 10 to 92 are calculated with an optical model program in which a previously determined complex nuclear potential is utilized. The dependence of the T_ℓ values, and hence of σ_R , on the Woods-Saxon parameters is investigated as a function of projectile energy. The optical model reaction cross sections are compared with those derived from (1) a square-well potential and (2) a model which approximates the real optical model potential barrier by a parabola and makes use of the Hill-Wheeler penetration formula for a parabolic potential.

I. INTRODUCTION

Shapiro⁽¹⁾ and Blatt and Weisskopf⁽²⁾ have calculated total reaction cross sections for alpha particles with a square-well potential. The total reaction cross section is given by

$$\sigma_R = \pi \lambda^2 \sum_{\ell=0}^{\infty} (2\ell+1) T_\ell(\epsilon) \quad , \quad (1)$$

where λ is the de Broglie wavelength, ℓ is the angular momentum of the incident particle in units of \hbar , and $T_\ell(\epsilon)$ is the transmission coefficient of the incident particle of energy ϵ . The transmission coefficients (actually $4/T_\ell$ are tabulated) for alpha particles derived from the square-well potential are available⁽³⁾ for target nuclei with $Z < 40$. Igo⁽⁴⁾ has calculated total reaction cross sections with a complex nuclear potential for six target nuclei with alpha-particle projectiles of a few energies. Transmission coefficients calculated with the complex nuclear potential are not available.

Since alpha-particle transmission coefficients for high-Z targets are not available, we have calculated this quantity for a large variety of targets at a number of alpha-particle energies with a complex nuclear potential. For the light-Z targets, the transmission coefficients derived with the complex nuclear potential of the optical model are compared with those previously calculated with the square-well potential.(3)

II. RESULTS AND DISCUSSION

The optical-model potential employed in these calculations is written as

$$V_{\ell}(r) = V_C + \frac{\ell(\ell+1)\hbar^2}{2M_\alpha r^2} + \frac{V}{1 + \exp\left(\frac{r-r_0}{d}\right)} + \frac{iW}{1 + \exp\left(\frac{r-r_0}{d}\right)} , \quad (2)$$

where V_C is the Coulomb potential, M_α the reduced mass of the alpha particle, and the third and fourth terms (in units of Mev) are the real and imaginary parts of the alpha-nucleus potential, respectively, exclusive of the Coulomb and centrifugal potentials. The Coulomb potential of the Hill-Ford(5) charge distribution was employed in Eq. (2). For alpha particles this is given by

$$V_C = \frac{2Ze^2}{r_C} \left[\frac{1}{n^2} + \frac{1}{2} - \frac{x^2}{6} + \frac{e^{-n}}{n^2} \left(\frac{1-e^{nx}}{nx} + \frac{e^{nx}}{2} \right) \right] \left/ \left(\frac{1}{3} + \frac{2}{n^2} + \frac{e^{-n}}{n^3} \right) \right. \text{(for } x < 1\text{)} \quad (3)$$

and

$$V_C = \frac{2Ze^2}{r_C} \left\{ \frac{1}{x} - \left[\frac{\left(\frac{1}{x} + \frac{n}{2} \right) e^{n-nx}}{e^{-n} + 2n + \frac{1}{3} n^3} \right] \right\} \text{(for } x > 1\text{)} , \quad (4)$$

where $x = r/r_C$ and where n is 10 for heavy elements and is proportional to $A^{1/3}$. The quantity r_C is the distance out to the half-value point of the charge distribution. The value $1.17A^{1/3} \times 10^{-13}$ cm for r_C was chosen larger than the value obtained from the electron-scattering experiments(6) to take into account roughly the effect of the finite size of the alpha-particle charge distribution.

The parameters V , W , r_0 , and d in the Woods-Saxon potential,(7)

$$(V + iW) / \left[1 + \exp\left(\frac{r-r_0}{d}\right) \right] ,$$

were chosen to reproduce the nuclear potential given by⁽⁴⁾

$$-1100 \exp \left[-\left(\frac{r-1.17A^{1/3}}{0.574} \right) \right] - 45.7 i \exp \left[-\left(\frac{r-1.40A^{1/3}}{0.578} \right) \right]$$

for values of r where the real part of the nuclear potential is greater than -10 Mev. The Woods-Saxon parameters for the nuclides which we investigated are given in Table I. The depth of the potential for small values of r is also fixed when the parameters of Table I are used, although it has been shown that alpha-particle scattering is not sensitive to the potential depth.

The total reaction cross sections σ_R and the transmission coefficients T_ℓ calculated with the parameters of Table I are listed in Tables II and III, respectively. It should be emphasized that the alpha-particle energies are given in the laboratory system.

Table I
WOODS-SAXON POTENTIAL PARAMETERS*

Nuclide	W(Mev)	n	Nuclide	W(Mev)	n
$^{10}\text{Ne}^{20}$	- 5.30	4.42	$^{37}\text{Rb}^{85}$	-13.30	7.16
$^{19}\text{K}^{41}$	- 8.70	5.60	$^{41}\text{Nb}^{93}$	-13.74	7.37
$^{22}\text{Ti}^{48}$	- 9.51	5.91	$^{45}\text{Rh}^{103}$	-14.30	7.62
$^{23}\text{V}^{51}$	-10.00	6.04	$^{50}\text{Sn}^{119}$	-16.20	8.00
$^{24}\text{Cr}^{52}$	- 9.90	6.07	$^{60}\text{Ni}^{144}$	-18.23	8.53
$^{25}\text{Mn}^{53}$	- 9.98	6.11	$^{70}\text{Yb}^{173}$	-20.79	9.07
$^{25}\text{Mn}^{55}$	-10.25	6.19	$^{78}\text{Pt}^{195}$	-22.10	9.44
$^{26}\text{Fe}^{56}$	-10.26	6.23	$^{82}\text{Pb}^{206}$	-23.00	9.61
$^{27}\text{Co}^{55}$	-10.17	6.19	$^{90}\text{Th}^{232}$	-26.11	10.00
$^{32}\text{Ge}^{72}$	-11.85	6.77	$^{92}\text{U}^{235}$	-27.00	10.04

* In all cases,

$$V(\text{Mev}) = -50$$

$$r_0(\text{fermi}) = 1.17A^{1/3} + 1.77$$

$$r_C(\text{fermi}) = 1.17A^{1/3}$$

and

$$d(\text{fermi}) = 0.576$$

Table II
THEORETICAL REACTION CROSS SECTIONS (σ_R) MILLIBARNS

E_{Lab} (Mev)	$^{10}Ne^{20}$	$^{19}K^{41}$	$^{22}Ti^{48}$	$^{23}V^{51}$	$^{24}Cr^{52}$	$^{25}Mn^{53}$	$^{25}Mn^{55}$	$^{26}Fe^{56}$	$^{27}Co^{55}$	$^{32}Ge^{72}$	$^{37}Rb^{85}$
2	0.36										
3	23.1										
4	177	0.44	0.035	0.016	0.0059	0.0022	0.0026	0.0010	0.0003		
6	608	70	16.9	10.5	5.49	2.85	3.28	1.68	0.741	0.053	0.0027
7	745		91.5		40.5	24.2		16.0	8.05		
8	862	422	250	205	150	105	116	79.0	46.5	8.17	0.91
9			435		320	257		216	151		
10	1017	744	603	562	496	431	452	388	307	140	35.0
11			745		650	589		551	469		
12		961	862	834	780	725	749	693	614	454	249
13			959		888	839		813	739		
14	1128	1104	1040	1024	980	935	960	914	844	736	555
16	1175			1159			1112				809
18		1280		1259			1224				1005
20	1170			1334			1310				
22		1376		1393			1377				1278
24	1200			1438				1469			
26		1429		1473						1471	1455
28				1501							
30	1186	1461		1524			1529			1566	1561
34		1482		1559			1570			1633	1663
38	1140	1495		1581			1599			1681	1727
42		1495		1595			1618			1716	1774
46	1081	1493		1603			1628			1742	1811

E_{Lab} (Mev)	$^{41}Nb^{93}$	$^{45}Rh^{103}$	$^{50}Sn^{119}$	$^{60}Nd^{144}$	$^{70}Yb^{173}$	$^{78}Pt^{195}$	$^{82}Pb^{206}$	$^{90}Th^{232}$	$^{92}U^{235}$
2									
3									
4									
6									
7									
8	0.13	0.021		0.00001					
9									
10	8.03	1.84	0.34	0.0086					
11									
12	109	39.2	11.0	0.491	0.026				0.000024
13									
14	384	238	111	10.1	0.818	0.10	0.036	0.0048	0.0026
16	663	525	371	94.0	11.8	1.96	0.79	0.148	0.091
18	885	773	646	324	93.0	20.4	8.75	1.62	0.966
20		971	873	590	310	124	67.7	18.0	11.7
22	1199	1130	1058	822	570	350	249	106	76.8
24									
26	1405	1365	1333	1015	804	602	498	312	257
28									
30	1547	1528	1526	1427	1315	1191	1123	996	945
34	1649	1647	1666	1611	1547	1461	1413	1328	1286
38	1724	1735	1772	1752	1724	1669	1636	1584	1550
42	1782	1802	1854	1861	1864	1832	1812	1787	1759
46	1826	1855	1918	1948	1975	1964	1953	1950	1928

Table III
T₁ (TRANSMISSION COEFFICIENT FOR ALPHA PARTICLES (IN MeV ON THE LABORATORY ENERGY SCALE)
 10^{480} (TARGET NUCLEUS)

ℓ	2	3	4	6	7	8	10	14	16	20	24	30	35	46	
0	7.704	7.582	5.551	9.461	9.521	9.491	9.451	9.461	9.471	9.481	9.441	9.361	9.241	9.141	
1	4.609	3.422	2.591	8.061	9.041	9.481	9.741	9.671	9.601	9.481	9.411	9.331	9.241	9.141	
2	1.323	1.752	2.411	8.541	9.011	9.141	9.261	9.401	9.451	9.471	9.431	9.341	9.221	9.121	
3	2.465	2.953	4.342	5.351	7.941	9.251	9.891	9.681	9.561	9.421	9.361	9.301	9.211	9.101	
4	2.986	6.484	1.602	3.541	5.691	7.031	8.371	9.291	9.431	9.471	9.401	9.291	9.171	9.051	
5		4.755	1.183	6.202	2.281	5.461	9.621	9.481	9.321	9.251	9.271	9.241	9.151	9.031	
6		6.356	2.144	1.302	4.612	1.191	4.131	9.171	9.671	9.571	9.341	9.181	9.031	9.001	
7			1.445	1.283	6.693	2.842	2.481	7.071	7.911	8.921	9.261	9.221	9.051	8.931	
8			1.896	1.524	6.944	2.473	2.042	4.921	9.071	9.181	8.861	8.971	8.491	8.891	
9				2.505	1.254	4.844	4.213	7.342	2.671	7.831	7.841	9.101	8.931	8.791	
10					4.166	2.142	7.932	6.365	1.762	7.502	3.201	6.341	9.161	8.981	8.701
11						4.286	1.735	1.454	2.653	8.323	8.152	5.611	7.191	8.631	8.751
12							3.872	3.676	7.304	2.153	1.112	6.522	7.671	8.101	8.341
13							1.046	9.600	2.214	6.684	2.703	1.402	1.031	9.261	8.531
14								2.569	6.625	2.103	6.753	4.013	2.652	2.001	8.771
15									2.115	6.395	1.564	1.143	8.943	5.672	2.061
16									6.576	1.825	3.275	2.94	3.003	2.152	8.562
17										6.106	7.015	9.374	8.542	3.522	
18										1.056	1.495	2.664	3.253	1.572	
19											2.829	6.775	1.143	6.892	
20												1.555	3.614	2.833	
21												3.246	1.634	1.162	
22													2.652	3.542	
23													6.156	1.094	
24													1.316	3.075	
25														7.536	
26														1.726	

10⁴¹ · TAF (T₁ L₁ S₁)

ℓ	4	6	8	10	12	14	16	22	26	30	34	38	42	46						
0	1.393	2.451	8.671	9.821	9.951	9.901	9.961	9.971	9.971	9.971	9.961	9.951	9.941	9.931						
1	1.043	2.051	8.041	9.571	9.841	9.591	9.941	9.651	9.971	9.691	9.981	9.951	9.941	9.931						
2	4.814	1.221	7.651	9.641	9.891	9.931	9.961	9.971	9.971	9.961	9.951	9.941	9.941	9.931						
3	1.864	5.862	5.771	9.101	9.831	9.731	9.971	9.971	9.971	9.961	9.951	9.951	9.941	9.931						
4	4.755	1.942	3.891	8.571	9.591	9.821	9.951	9.951	9.971	9.971	9.961	9.951	9.931	9.921						
5	1.145	5.113	1.451	6.631	9.351	9.911	9.961	9.971	9.971	9.951	9.951	9.951	9.941	9.921						
6	2.209	1.133	4.752	3.831	7.551	9.331	9.961	9.971	9.971	9.971	9.941	9.931	9.921	9.911						
7		2.134	9.493	1.311	5.731	8.771	9.741	9.911	9.961	9.951	9.941	9.921	9.911	9.901						
8		4.425	2.033	2.592	2.621	6.971	9.821	9.921	9.961	9.971	9.931	9.921	9.911	9.891						
9		9.116	4.154	6.573	5.762	2.641	8.401	9.901	9.971	9.931	9.961	9.901	9.891	9.891						
10			1.996	2.542	1.363	1.122	6.932	6.311	9.131	9.791	9.941	9.931	9.901	9.881	9.871					
11				2.415	3.524	2.653	1.442	2.301	8.41	9.591	9.741	9.851	9.861	9.881	1.861					
12					6.146	9.775	1.474	3.862	5.592	4.011	9.151	9.921	9.811	9.801	9.831	9.841				
13						1.596	2.323	2.284	1.142	1.452	1.321	5.201	9.001	9.331	9.821	9.791				
14							8.169	7.145	3.784	4.083	3.312	2.191	6.181	8.691	9.731	9.921	9.851			
15								2.336	2.275	1.294	1.273	1.012	5.252	2.671	7.141	8.701	9.411	9.751		
16									7.066	4.405	3.864	3.593	1.752	6.712	2.621	7.441	9.191	9.321		
17										1.515	1.894	1.263	6.823	2.442	7.532	2.332	6.431	9.611		
18										5.096	2.835	4.194	2.693	1.032	2.972	7.772	2.001	4.931		
19											6.586	1.284	1.013	4.403	1.332	3.302	7.602	1.701		
20											1.406	3.585	3.534	1.823	6.073	1.552	3.452	7.182		
21												9.149	1.134	7.074	2.713	7.483	1.692	3.442		
22													2.126	3.315	2.534	1.153	3.553	8.503	1.752	
23														8.846	8.295	4.484	1.614	6.764	2.023	4.732
24															2.485	1.614	6.764			
25															6.806	5.315	2.634	9.064	2.373	
26																1.736	1.605	9.355	3.754	1.123
27																	3.055	1.434	4.874	
28																	9.116	4.075	1.964	
29																		1.595	7.225	
30																		4.656	2.445	
31																		1.306	7.616	

*The underlined number is the negative exponent of 10 by which the three-digit number is to be multiplied, e.g., the entry 7.704 indicates 7.70×10^{-4} .

Table III (Cont'd.)
 ^{227}Ra TARGET NUCLEUS

ℓ	4	6	7	8	9	10	11	12	13	14
0	1.074	6.612	3.321	6.891	8.791	9.501	9.761	9.881	9.911	9.941
1	8.005	5.142	2.711	6.151	8.371	9.331	9.721	9.891	9.961	9.991
2	4.055	3.002	1.911	5.301	7.361	9.131	9.581	9.771	9.861	9.911
3	1.645	1.352	9.692	3.461	6.581	8.531	9.411	9.761	9.901	9.961
4	4.995	4.723	4.042	1.881	4.741	7.301	8.691	9.341	9.651	9.811
5	1.316	1.303	1.192	6.602	2.341	5.161	7.621	8.951	9.521	9.761
6		3.224	3.183	1.972	8.342	2.421	4.831	7.071	8.511	9.291
7		7.045	6.954	4.533	2.192	8.122	2.261	4.531	6.701	8.131
8		1.625	1.594	1.023	4.873	1.872	5.992	1.601	3.431	5.721
9		3.789	3.755	2.394	1.153	4.473	1.492	4.282	1.061	2.251
10				9.176	5.925	2.774	1.043	3.383	9.893	2.672
11				2.296	1.575	7.505	2.804	8.774	2.423	6.133
12					4.146	2.095	8.095	2.574	7.054	1.743
13					1.076	5.886	2.395	7.842	2.194	5.434
14						1.606	7.036	2.432	7.062	1.744
15							2.036	7.496	2.285	6.025
16								2.216	7.276	2.025
17									0.756	1.715
18										5.786

 ^{23}V TARGET NUCLEUS

ℓ	4	6	8	10	12	14	16	18	20	22	24	26	28	30	34	38	42	46	
0	4.725	4.132	6.111	9.341	9.831	9.941	9.981	10.001	10.001	10.001	10.001	9.991	9.991	9.991	9.981	9.931	9.381		
1	3.525	3.162	5.411	9.211	9.871	9.981	9.991	9.981	9.992	9.991	9.991	9.991	9.991	9.991	9.981	9.981	9.981		
2	1.855	1.872	4.471	8.891	9.741	9.921	9.971	9.991	10.001	10.001	10.001	9.991	9.991	9.991	9.981	9.981	9.981		
3	7.756	8.372	2.821	8.271	9.711	9.941	9.971	9.981	9.981	9.991	9.991	9.991	9.991	9.991	9.981	9.981	9.981		
4	2.406	3.023	1.451	6.841	9.271	9.821	9.961	9.991	10.001	10.001	9.991	9.991	9.991	9.991	9.981	9.981	9.981		
5		8.564	5.142	4.691	8.751	9.691	9.881	9.941	9.971	9.981	9.991	9.991	9.991	9.991	9.981	9.931	9.971		
6		2.214	1.522	2.111	6.871	9.281	9.861	9.971	9.981	9.981	9.981	9.981	9.981	9.981	9.981	9.981	9.971		
7		5.125	3.693	7.072	4.211	7.981	9.381	9.811	9.951	9.991	10.001	9.991	9.991	9.981	9.971	9.971	9.971		
8		1.215	8.544	1.692	1.532	5.631	8.691	9.571	9.811	9.901	9.941	9.971	9.981	9.991	9.971	9.971	9.961		
9		2.936	2.084	4.103	4.062	2.231	6.031	8.801	9.721	9.921	9.951	9.951	9.951	9.961	9.971	9.971	9.961		
10			5.205	9.984	9.903	6.652	2.751	6.091	8.451	9.511	9.891	9.991	10.001	9.991	9.961	9.961	9.961		
11			1.425	2.724	2.473	1.552	7.632	2.901	6.201	9.391	9.251	9.601	9.861	9.951	9.991	9.971	9.941		
12			3.819	7.972	7.264	4.223	1.922	7.512	2.461	5.661	8.291	9.321	9.631	9.761	9.901	9.951	9.961	9.951	
13			1.029	2.362	2.334	1.323	5.693	2.032	6.762	1.911	4.361	7.271	9.121	9.751	9.881	9.881	9.911	9.931	
14				7.159	7.375	4.424	1.873	6.453	1.992	5.752	1.511	3.291	5.711	7.011	9.831	9.981	9.911	9.891	
15				2.156	2.405	1.544	6.724	2.293	6.603	1.732	4.382	1.091	2.491	4.561	8.131	9.671	9.991	9.951	
16					7.726	5.385	2.484	8.894	2.523	6.273	1.472	3.292	7.132	1.571	5.531	8.381	9.461	9.971	
17						9.195	3.334	1.013	2.443	5.903	1.252	2.492	4.852	1.861	5.921	8.791	9.381		
18						3.425	1.264	4.054	9.324	2.503	5.293	1.042	1.942	6.182	1.441	5.571	9.081		
19						4.655	1.624	3.984	1.093	2.343	4.563	8.603	2.602	7.082	1.881	4.781			
20							1.625	6.275	1.154	4.734	1.053	2.003	3.923	1.202	3.132	7.532	1.751		
21								5.376	2.338	3.585	2.074	4.704	8.434	1.763	5.763	1.512	3.562	7.602	
22									9.072	2.104	3.354	7.584	2.763	7.513	1.752	3.702			
23										3.985	9.195	1.244	3.074	1.293	3.783	8.932	1.912		
24												1.164	5.714	1.873	4.693	1.012			
25													4.015	2.374	8.904	2.433	5.433		
26													1.285	9.115	4.004	1.222	2.923		
27															5.874	1.543			
28																7.774			
29																3.714			
30																1.654			
31																6.765			

Table III (Cont'd.)
 $^{24}\text{Cr}^{52}$ (TARGET NUCLEUS)

25Mn⁵³(TARGET NUCLEUS)

Table III (Cont'd.)
 $^{25}\text{Mn}^{55}$ (TARGET NUCLEUS)

ℓ	4	6	8	10	12	14	16	18	20	22	26	30	34	38	42	46									
0	7.426	1.292	4.131	8.871	9.751	9.931	9.981	10.001	10.001	10.001	10.001	9.991	9.991	9.991	9.991	9.981									
1	5.596	9.903	3.511	8.691	9.781	9.951	9.981	9.991	9.991	9.991	9.991	9.991	9.991	9.991	9.991	9.981									
2	3.066	5.853	2.661	8.191	9.621	9.901	9.971	10.001	10.001	10.001	9.991	9.991	9.991	9.991	9.991	9.981									
3	1.406	2.673	1.521	7.291	9.521	9.891	9.961	9.981	9.981	9.991	10.001	9.991	9.991	9.991	9.991	9.981									
4	5.227	9.914	7.162	5.511	8.951	9.771	9.951	9.991	10.001	10.001	9.991	9.991	9.991	9.991	9.991	9.981									
5		2.984	2.482	3.331	8.121	9.541	9.841	9.931	9.971	9.991	10.001	9.991	9.991	9.991	9.981	9.981									
6		8.215	7.363	1.341	5.941	9.031	9.801	9.941	9.971	9.981	9.981	9.991	9.991	9.991	9.981	9.981									
7		2.065	1.893	4.302	3.221	7.411	9.251	9.791	9.951	10.001	9.991	9.981	9.981	9.981	9.981	9.981									
8		5.206	4.664	1.062	1.111	4.841	8.301	9.451	9.781	9.901	9.981	9.991	9.991	9.981	9.981	9.971									
9		1.296	1.214	2.693	2.922	1.811	5.561	8.621	9.651	9.881	9.941	9.971	9.981	9.981	9.981	9.971									
10			3.225	6.964	7.453	5.292	2.371	5.751	8.391	9.531	9.991	9.981	9.971	9.971	9.971	9.971									
11				8.926	1.974	1.953	1.302	6.912	2.661	5.901	8.191	9.711	9.981	9.991	9.971	9.961									
12					2.386	5.885	5.894	3.643	1.742	7.142	2.441	5.651	9.221	9.771	9.941	9.981	9.961								
13						1.785	1.894	1.163	5.263	1.982	6.682	1.971	7.561	9.701	9.851	9.901	9.941	9.951							
14							6.195	3.964	1.763	6.133	2.002	5.932	3.491	8.331	9.891	9.941	9.911	9.921							
15								2.035	1.394	6.384	2.063	6.573	1.822	1.211	4.831	8.531	9.861	10.001	9.941						
16									6.536	4.895	2.374	7.014	2.383	6.563	3.592	1.871	5.891	8.611	9.681	9.961					
17										1.715	8.875	2.294	8.624	2.533	1.282	5.662	2.331	6.611	8.821	9.521					
18											5.886	3.305	6.955	2.974	9.634	4.883	2.162	7.442	2.501	6.741	9.171				
19												1.955	9.555	3.474	1.803	8.943	3.022	8.672	2.451	6.181					
20													5.046	2.835	1.174	6.234	3.653	1.342	3.732	9.312	2.281				
21														1.186	7.746	3.625	1.994	1.413	5.903	1.752	4.232	9.472			
22																5.815	5.034	2.493	8.213	2.072	4.522				
23																1.565	1.654	9.764	3.713	1.032	2.302				
24																	4.985	3.534	1.573	4.923	1.192				
25																		1.375	1.184	6.184	2.233	5.983			
26																		3.496	3.585	2.234	9.344	2.853			
27																			9.996	7.395	3.624	1.273			
28																			2.566	2.255	1.294	5.204			
29																			6.286	4.195	1.964				
30																			1.636	1.265	6.815				
31																				3.516	2.175				
32																					6.416				
33																					1.756				

Table III (Cont'd.)
 ^{56}Fe (TARGET NUCLEUS)

$^{27}\text{Co}^{55}$ (TARGET NUCLEUS)

Table III (Cont'd.)
 $^{32}\text{Ge}^{72}$ (TARGET NUCLEUS)

\mathcal{L}	6	8	10	12	14	18	22	26	30	34	38	42	46
0	1.814	3.492	4.871	8.971	9.791	9.991	10.001	10.001	10.001	10.001	10.001	10.001	10.001
1	1.444	2.822	4.441	8.851	9.761	9.981	10.001	10.001	10.001	10.001	10.001	10.001	10.001
2	9.145	1.882	3.561	8.461	9.701	9.981	10.001	10.001	10.001	10.001	10.001	10.001	10.001
3	4.735	1.022	2.451	7.801	9.541	9.961	10.001	10.001	10.001	10.001	10.001	10.001	10.001
4	2.075	4.583	1.361	6.521	9.261	9.951	9.991	10.001	10.001	10.001	10.001	10.001	10.001
5	7.846	1.753	6.132	4.631	8.561	9.911	9.991	10.001	10.001	10.001	10.001	10.001	10.001
6	2.706	5.974	2.232	2.511	7.281	9.811	9.981	10.001	10.001	10.001	10.001	10.001	10.001
7	8.947	1.904	7.263	1.011	4.881	9.631	9.961	9.991	10.001	10.001	10.001	10.001	10.001
8	5.865	2.173	3.322	2.401	8.961	9.921	10.001	10.001	10.001	10.001	10.001	10.001	10.001
9	1.805	6.514	9.633	8.272	7.571	9.741	9.961	10.001	10.001	10.001	10.001	9.991	9.991
10	5.426	2.024	2.843	2.412	4.691	9.411	9.911	9.971	9.991	10.001	10.001	10.001	9.991
11	1.576	6.395	8.694	6.793	1.931	8.041	9.831	9.981	9.981	9.991	9.991	9.991	9.991
12		2.045	2.774	1.933	6.062	5.311	9.221	9.921	10.001	9.991	9.991	9.991	9.991
13		6.436	8.865	5.634	1.762	2.251	7.821	9.611	9.931	10.001	10.001	9.991	9.991
14		1.926	2.755	1.614	5.633	6.972	4.611	9.001	9.781	9.931	9.981	9.991	9.991
15			8.116	4.355	1.873	2.292	1.711	6.481	9.491	9.901	9.941	9.971	
16			2.256	1.105	6.174	8.103	5.762	3.011	7.541	9.671	9.971	9.961	
17				2.576	1.944	3.033	2.072	1.081	4.271	8.091	9.671	9.991	
18					5.685	1.123	8.323	3.882	1.631	5.261	8.431	9.601	
19					1.545	3.904	3.433	1.632	5.932	2.081	5.881	8.711	
20					3.806	1.274	1.373	7.223	2.572	7.882	2.371	6.071	
21						3.825	5.144	3.183	1.202	3.522	9.452	2.481	
22						1.065	1.804	1.343	5.673	1.712	4.382	1.051	
23						2.726	5.825	5.294	2.613	8.513	2.192	5.052	
24							1.735	1.944	1.143	4.173	1.132	2.602	
25								4.766	6.595	4.634	1.973	5.843	1.392
26								1.236	2.065	1.754	8.734	2.933	7.443
27										6.115	3.614	1.403	3.913
28										1.975	1.394	6.234	1.973
29											4.905	2.584	9.394
30											1.605	9.925	4.164
31											4.866	3.515	1.714
32												1.155	6.525
33												3.516	2.305

Table III (Cont'd.)

 $^{37}\text{Rb}^{85}$ (TARGET NUCLEUS)

ℓ	6	8	10	12	14	16	18	22	26	30	34	38	42	46	
0	8.036	3.613	1.501	7.081	9.431	9.871	9.961	9.991	10.001	10.001	10.001	10.001	10.001	10.001	
1	6.596	2.972	1.291	6.771	9.351	9.851	9.961	10.001	10.001	10.001	10.001	10.001	10.001	10.001	
2	4.446	2.023	9.412	6.071	9.181	9.821	9.951	9.991	10.001	10.001	10.001	10.001	10.001	10.001	
3	2.586	1.153	5.822	4.961	8.821	9.741	9.931	9.991	10.001	10.001	10.001	10.001	10.001	10.001	
4	1.276	5.594	3.012	3.481	8.161	9.591	9.891	9.991	10.001	10.001	10.001	10.001	10.001	10.001	
5	5.247	2.344	1.342	2.001	6.911	9.211	9.821	9.981	10.001	10.001	10.001	10.001	10.001	10.001	
6		9.265	5.193	9.232	5.001	8.591	9.641	9.971	10.001	10.001	10.001	10.001	10.001	10.001	
7		3.375	1.853	3.532	2.771	7.211	9.271	9.931	9.991	10.001	10.001	10.001	10.001	10.001	
8		1.172	6.314	1.212	1.161	4.851	8.301	9.871	9.981	9.991	10.001	10.001	10.001	10.001	
9		3.896	2.124	3.903	3.952	2.391	6.351	9.641	9.971	10.001	10.001	10.001	10.001	10.001	
10		1.236	7.295	1.273	1.212	8.622	3.561	9.111	9.891	9.981	10.001	10.001	10.001	10.001	
11		2.445	4.164	3.593	2.712	1.391	7.641	9.761	9.961	9.991	10.001	10.001	10.001	10.001	
12			1.374	1.063	8.263	4.522	4.791	9.211	9.921	9.981	10.001	10.001	10.001	10.001	
13			4.415	3.084	2.543	1.402	2.081	7.661	9.681	9.971	10.001	9.991	9.991	10.001	
14			1.365	8.615	7.894	4.533	6.912	4.791	8.991	9.821	9.981	10.001	10.001	10.001	
15				3.896	2.265	2.374	1.493	2.312	1.931	7.041	9.511	9.891	9.971	10.001	
16				1.066	5.546	6.755	4.784	8.253	6.782	3.591	8.301	9.751	9.931	9.971	
17						1.795	1.454	3.013	2.482	1.211	5.241	8.891	9.861	9.971	
18						4.446	4.135	1.083	9.763	3.542	2.341	6.401	9.141	9.401	
19								3.654	3.913	1.032	8.802	3.241	7.181	9.251	
20								1.154	1.523	3.033	3.662	1.251	3.941	7.691	
21										3.385	5.574	8.534	1.672	5.342	
22										1.903	2.254	7.753	2.532	6.942	
23										5.995	5.515	3.493	1.242	3.932	
24											1.255	1.493	5.973	1.722	4.152
25											2.596	5.904	2.773	8.793	2.182
26											4.957	2.214	1.213	4.353	1.162
27													4.924	2.043	6.043
28													1.854	8.984	3.023
29													6.465	3.674	1.423
30													2.095	1.394	6.214
31													6.236	4.875	2.534
32														1.585	9.515
33														4.806	3.325

 $^{41}\text{Nb}^{93}$ (TARGET NUCLEUS)

ℓ	8	10	12	14	16	18	22	26	30	34	38	42	46								
0	4.724	3.532	4.201	8.641	9.711	9.931	9.991	10.001	10.001	10.001	10.001	10.001	10.001								
1	3.944	2.992	3.841	8.471	9.671	9.921	9.991	10.001	10.001	10.001	10.001	10.001	10.001								
2	2.764	2.152	3.141	8.101	9.601	9.901	9.991	10.001	10.001	10.001	10.001	10.001	10.001								
3	1.654	1.312	2.251	7.401	9.431	9.861	9.991	10.001	10.001	10.001	10.001	10.001	10.001								
4	8.595	6.853	1.361	6.261	9.121	9.781	9.981	10.001	10.001	10.001	10.001	10.001	10.001								
5	3.975	3.153	6.932	4.591	8.501	9.641	9.971	9.991	10.001	10.001	10.001	10.001	10.001								
6	1.685	1.303	2.972	2.751	7.321	9.311	9.951	9.991	10.001	10.001	10.001	10.001	10.001								
7	6.626	5.044	1.112	1.291	5.371	8.631	8.891	9.991	10.001	10.001	10.001	10.001	10.001								
8	2.446	1.884	3.753	4.992	3.021	7.151	9.781	9.971	9.991	10.001	10.001	10.001	10.001								
9	8.607	6.845	1.173	1.682	1.291	4.761	9.441	9.951	9.991	10.001	10.001	10.001	10.001								
10		2.465	3.504	5.293	4.472	2.301	8.621	9.851	9.981	10.001	10.001	10.001	10.001								
11		8.506	9.935	1.623	1.432	8.392	6.722	9.641	9.951	9.991	10.001	10.001	10.001								
12			2.705	4.854	4.493	2.752	3.801	8.941	8.891	9.981	9.991	10.001	10.001								
13			6.866	1.404	1.403	8.793	1.541	7.101	9.611	9.961	9.991	9.991	10.001								
14			1.636	3.855	4.314	2.873	5.212	4.161	8.761	9.811	9.981	10.001	10.001								
15						9.946	1.274	9.364	1.782	1.661	6.711	9.421	9.891	9.981							
16							2.356	3.525	2.942	6.383	5.912	3.441	8.221	9.711	9.921						
17								9.036	8.705	2.303	2.202	1.351	5.231	8.951	9.851						
18									2.196	2.405	8.024	8.583	5.092	2.361	6.561	9.281					
19											2.644	3.383	2.072	9.172	3.441	7.421					
20												8.125	1.283	8.843	3.812	1.381	4.361	7.961			
21													2.325	4.564	3.733	1.722	5.842	1.831	5.001		
22														6.116	1.524	1.503	7.823	2.732	7.892	2.181	
23															1.466	4.665	5.644	3.463	1.322	3.802	9.712
24																1.984	1.453	6.283	1.922	4.802	
25																6.415	5.644	2.863	9.663	2.512	
26																1.935	2.054	1.223	4.713	1.322	
27																	6.875	4.874	2.173	6.793	
28																	2.135	1.804	9.374	3.343	
29																	6.165	3.764	1.543		
30																	1.965	1.404	6.654		
31																	5.756	4.835	2.664		
32																	1.555	9.865			
33																	4.616	3.395	1.085		
34																		3.236			
35																					

Table III (Cont'd.)

^{119}Sn TARGET NUCLEUS

Table III (Cont'd.)
 $^{60}\text{Nd}^{144}$ (TARGET NUCLEUS)

Table III (Cont'd.)

$^{70}\text{Yb}^{173}$ (TARGET NUCLEUS)

78Pt¹⁹⁵(CHART 1 NUCLEUS)

Table III (Cont'd.)

 $^{82}\text{Pb}^{206}$ (TARGET NUCLEUS)

ℓ	14	16	18	20	22	24	26	30	34	38	42	46
0	1.134	2.883	3.872	2.781	7.121	9.221	9.781	9.981	10.001	10.001	10.001	10.001
1	1.044	2.643	3.542	2.611	6.951	9.161	9.771	9.951	10.001	10.001	10.001	10.001
2	8.835	2.233	2.982	2.291	6.601	9.041	9.741	9.971	10.001	10.001	10.001	10.001
3	6.945	1.743	2.292	1.871	6.051	8.831	9.681	9.971	10.001	10.001	10.001	10.001
4	5.075	1.263	1.622	1.411	5.261	8.491	9.581	9.961	9.991	10.001	10.001	10.001
5	3.465	8.494	1.062	9.732	4.271	7.951	9.421	9.941	9.991	10.001	10.001	10.001
6	2.205	5.414	6.423	6.182	3.171	7.131	9.141	9.921	9.991	10.001	10.001	10.001
7	1.335	3.274	3.633	3.632	2.121	5.961	8.671	9.871	9.981	10.001	10.001	10.001
8	7.566	1.894	1.933	1.992	1.281	4.491	7.881	9.801	9.971	10.001	10.001	10.001
9	4.086	1.054	9.674	1.032	7.002	2.981	6.641	9.641	9.961	9.991	10.001	10.001
10	2.076	5.605	4.584	5.033	3.582	1.731	4.971	9.351	9.921	9.991	10.001	10.001
11	1.056	2.885	2.064	2.403	1.742	9.012	3.181	8.771	9.861	9.981	10.001	10.001
12		1.435	8.735	1.093	8.203	4.392	1.761	7.681	9.721	9.961	9.991	10.001
13		6.846	3.505	4.734	3.753	2.062	8.732	5.921	9.411	9.921	9.991	10.001
14		1.325	1.964	1.663	9.463	4.112	3.821	8.731	9.831	9.971	10.001	
15		4.676	7.682	7.094	4.263	1.902	2.071	7.411	9.611	9.941	9.991	
16		1.586	2.855	2.894	1.873	8.673	1.011	5.341	9.101	9.871	9.981	
17			10.006	1.124	7.924	3.903	4.712	3.141	7.981	9.671	9.951	
18				3.276	4.125	3.214	1.713	2.212	1.591	6.021	9.191	9.871
19					1.435	1.234	7.184	1.032	7.602	3.681	8.071	9.651
20						4.676	4.485	2.884	4.793	3.652	1.911	6.051
21							1.416	1.545	1.004	2.163	1.782	9.332
22								4.946	3.925	9.324	8.643	4.612
23									1.516	1.325	3.824	4.113
24										4.206	1.484	1.893
25											1.276	5.135
26												1.875
27												6.006
28												1.846
29												1.695
30												5.486
31												1.686
32												1.125
33												3.616
34												4.925
35												1.574
36												6.105
												2.245

 $^{90}\text{Th}^{232}$ (TARGET NUCLEUS)

ℓ	14	16	18	20	22	24	26	30	34	38	42	46
0	1.425	4.334	6.973	7.872	3.971	7.841	9.401	9.941	9.991	10.001	10.001	10.001
1	1.325	4.454	6.403	7.302	3.791	7.721	9.361	9.941	9.991	10.001	10.001	10.001
2	1.145	3.864	5.403	6.282	3.441	7.461	9.271	9.931	9.991	10.001	10.001	10.001
3	9.096	3.104	4.203	5.002	2.941	7.031	9.131	9.921	9.991	10.001	10.001	10.001
4	6.806	2.324	3.013	3.682	2.351	6.401	8.891	9.901	9.991	10.001	10.001	10.001
5	4.746	1.644	2.003	2.522	1.741	5.541	8.521	9.861	9.981	10.001	10.001	10.001
6	3.066	1.094	1.233	1.602	1.191	4.481	7.931	9.811	9.981	10.001	10.001	10.001
7	1.886	6.875	7.094	9.533	7.482	3.311	7.061	9.711	9.961	9.991	10.001	10.001
8	1.106	4.115	3.814	5.323	4.382	2.211	5.841	9.541	9.951	9.991	10.001	10.001
9		2.355	1.924	2.813	2.402	1.341	4.371	9.231	9.911	9.991	10.001	10.001
10		1.295	9.075	1.413	1.252	7.422	2.881	8.671	9.851	9.981	10.001	10.001
11			6.676	4.035	6.674	6.223	3.652	1.691	7.711	9.731	9.961	9.991
12				3.366	1.685	3.004	2.963	1.912	8.962	6.211	9.481	9.931
13					1.606	6.606	1.264	1.353	9.143	4.472	4.341	8.971
14							5.165	5.914	4.233	2.152	2.591	8.001
15								1.965	2.464	1.893	1.012	1.361
16									7.036	9.725	9.114	4.583
17										3.635	3.324	2.023
18										1.285	1.294	8.584
19											4.765	3.474
20											1.665	1.334
21												5.426
22												1.665
23												5.376
24												8.255
25												2.885
26												9.506
27												2.966
28												3.035
29												1.754
30												6.475
31												2.265
32												1.044
33												3.795
34												1.305
35												4.176
36												1.296
												1.815

Table III (Cont'd.)
 $^{92}\text{U}^{235}$ (TARGET NUCLEUS)

ℓ	12	14	16	18	20	22	24	26	30	34	38	42	46				
0	1.197	7.816	2.894	4.133	5.132	3.051	7.161	9.181	9.921	9.991	10.001	10.001	10.001				
1	1.197	7.236	2.694	3.793	4.752	2.891	7.011	9.121	9.921	9.991	10.001	10.001	10.001				
2	2.988	6.276	2.334	3.213	4.072	2.581	6.701	9.011	9.911	9.991	10.001	10.001	10.001				
3		5.016	1.884	2.503	3.242	2.171	6.211	8.821	9.891	9.991	10.001	10.001	10.001				
4		3.766	1.424	1.803	2.382	1.701	5.521	8.521	9.861	9.981	10.001	10.001	10.001				
5		2.616	1.014	1.203	1.632	1.241	4.641	8.041	9.821	9.981	10.001	10.001	10.001				
6		1.696	6.765	7.394	1.042	8.342	3.611	7.331	9.741	9.971	10.001	10.001	10.001				
7		1.056	4.285	4.264	6.213	5.222	2.581	6.331	9.611	9.951	9.991	10.001	10.001				
8			2.585	2.294	3.483	3.052	1.671	5.041	9.391	9.931	9.991	10.001	10.001				
9			1.485	1.154	1.843	1.682	9.932	3.611	9.001	9.891	9.981	10.001	10.001				
10			8.116	5.445	9.224	8.763	5.472	2.291	8.311	9.811	9.971	10.001	10.001				
11			4.246	2.415	4.374	4.373	2.842	1.311	7.181	9.651	9.951	9.991	10.001				
12			2.116	9.976	1.964	2.083	1.422	6.912	5.571	9.341	9.911	9.991	10.001				
13				3.906	8.335	9.504	6.783	3.452	3.731	8.731	9.831	9.971	10.001				
14					3.345	4.134	3.143	1.672	2.161	7.601	9.651	9.951	9.991				
15						1.265	1.714	1.403	7.813	1.131	5.851	9.271	9.891	9.981			
16							4.536	6.705	5.974	3.563	5.542	3.821	8.471	9.761	9.961		
17								2.485	2.424	1.563	2.662	2.141	7.001	9.461	9.911		
18								8.666	9.345	6.574	1.262	1.091	4.931	8.791	9.791		
19									3.415	2.634	5.833	5.382	2.921	7.441	9.501		
20									1.175	10.005	2.613	2.632	1.541	5.391	8.821		
21										3.766	3.595	1.123	1.272	7.792	3.271	7.431	
22											1.225	4.584	5.993	3.932	1.761	5.321	
23											3.886	1.784	2.733	1.972	9.102	3.201	
24												6.505	1.193	9.743	4.732	1.731	
25													2.255	4.914	4.663	2.462	9.202
26													7.316	1.924	2.133	1.262	4.932
27														7.075	9.294	6.283	2.652
28														2.465	3.834	3.003	1.402
29															1.494	1.363	7.223
30															5.455	5.844	3.563
31															1.885	2.374	1.673
32																9.045	7.384
33																3.255	3.084
34																1.105	1.214
35																3.526	4.505
36																1.056	1.575

Several calculations were made in which all the parameters were fixed, except n , in the Hill-Ford charge distribution. The results showed that the reaction cross section is rather insensitive to changes in the charge distribution. For a fixed set of Woods-Saxon parameters, the relative cross sections for 22-Mev alpha particles on silver were in the ratio 1.000:1.000:1.043 for $n = 20, 7.75$ and 3, respectively.

A. Simplified Calculation of Reaction Cross Sections with a Parabolic Approximation of Optical Model Real Potential

Values of T_ℓ and σ_R have also been calculated with a model⁽⁸⁾ which embraces some simplifying assumptions and as a result greatly reduces the computational problem. The potential function given by

$$V_\ell(r) = \frac{2Ze^2}{r} + \frac{\ell(\ell+1)\hbar^2}{2M_\alpha r^2} - 1100 \exp\left[-\left(\frac{r-1.17A^{1/3}}{0.574}\right)\right] , \quad (5)$$

which describes the real part of the barrier [Eq. (5)], is approximated by a parabola. The transmission coefficients T_ℓ for a parabolic potential⁽⁹⁾ are given by

$$T_\ell = \frac{1}{1 + \exp\left[\frac{2(B_\ell - E)}{\hbar\omega_\ell}\right]} , \quad (6)$$

where B_ℓ is the height of the barrier for angular momentum ℓ , E is the center of mass energy, and ω_ℓ is the vibrational frequency of the harmonic oscillator having a potential energy function given by the negative of the potential energy function describing the barrier.

The quantity $\hbar\omega_\ell$ in Eq. (6) is fixed by the curvature of the top of the barrier and the reduced mass of the system, and is given by

$$\hbar\omega_\ell = \left| \frac{\hbar^2}{M_\alpha} \frac{d^2V_\ell}{dr^2} \right|^{1/2} \quad (7)$$

where d^2V_ℓ/dr^2 is the second derivative of the real part of the barrier (Eq. 5) evaluated for the value of r for which $V_\ell(r)$ is a maximum.

B. Comparison of Reaction Cross Sections from Various Models

The alpha-particle barriers of U^{235} for the square-well potential, optical-model potential, and the parabolic approximation to the real part of

the optical-model potential are plotted in Fig. 1 for $\ell = 0$ and in Fig. 2 for $\ell = 25$. The square-well potential (curve a) includes the Coulomb and centrifugal barriers and a constant nuclear potential of -50 Mev for $r < (1.50A^{1/3} + 1.21)$ fermi and 0 for $r > (1.50A^{1/3} + 1.21)$ fermi.

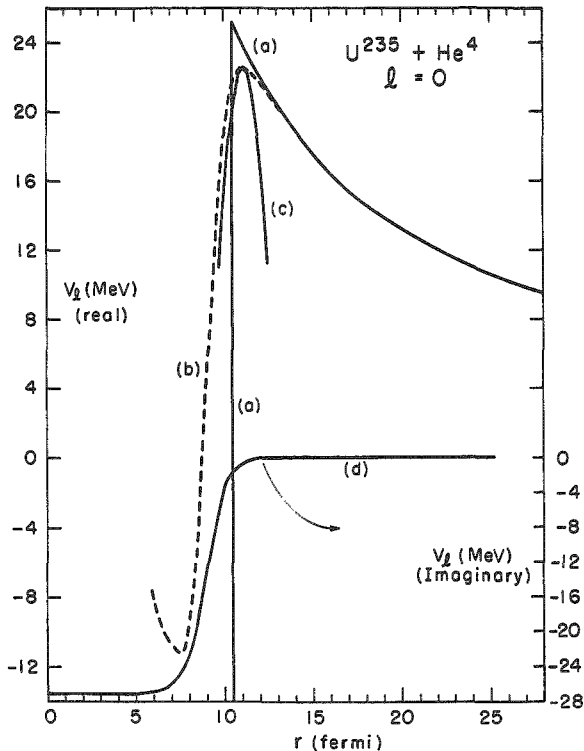


Fig. 1

Potential barriers for the reaction $_{92}\text{U}^{235} + {}_2\text{He}^4$ for angular momentum $\ell = 0$. (a) square-well potential for radius equal to $(1.50A^{1/3} + 1.21)$ fermi and a constant nuclear potential of $V = -50$ Mev for $r < (1.50A^{1/3} + 1.21)$ fermi and $V = 0$ for $r > (1.50A^{1/3} + 1.21)$ fermi. (b) Optical-model potential (real part) given by Eq. (2) with a nuclear potential equal to

$$-50 / \left[1 + \exp \left(\frac{r - 1.17A^{1/3} - 1.77}{0.576} \right) \right].$$

(c) Parabolic approximation of the real part of the optical-model potential [see Eqs. (5), (6), and (7) in text]. (d) Imaginary part of the optical-model potential which is given by

$$-27i / \left[1 + \exp \left(\frac{r - 1.17A^{1/3} - 1.77}{0.576} \right) \right].$$

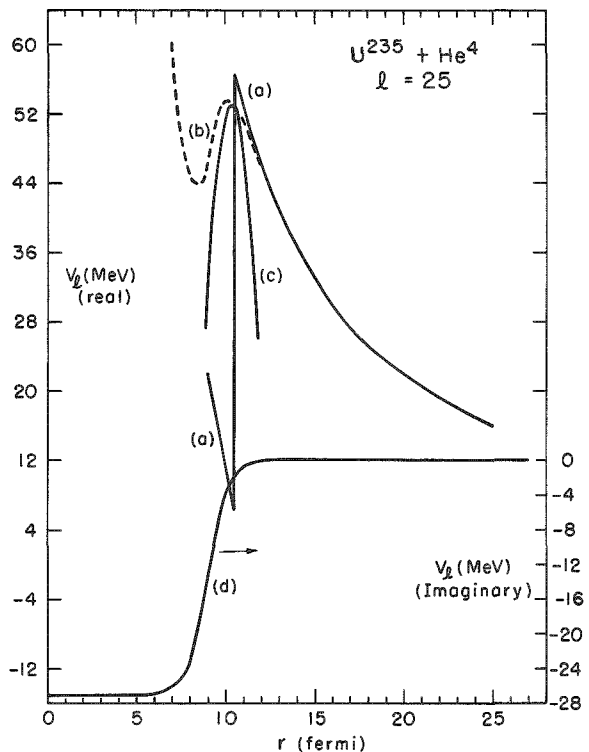


Fig. 2

Potential barriers for the reaction ${}_{92}\text{U}^{235} + {}_2\text{He}^4$ for angular momentum $\ell = 25$. See caption of Fig. 1 for description.

The real part of the optical-model potential for uranium (curve b) is calculated from Eq. (2) where the nuclear potential is given by

$$-50 \left/ \left[1 + \exp \left(\frac{r - 1.17A^{1/3} - 1.77}{0.576} \right) \right] \right..$$

The imaginary part of the optical model potential for uranium (curve d) is given by

$$-27i \left/ \left[1 + \exp \left(\frac{r - 1.17A^{1/3} - 1.77}{0.576} \right) \right] \right..$$

and these calculated values are also plotted in the above figures. The parabolic approximation to the real part of the optical-model potential (curve c) is calculated from Eqs. (5) and (7).

The maximum in the real part of the optical-model potential moves to smaller radii for increasing values of the angular momentum, whereas the imaginary part of the optical-model potential is independent of angular momentum. Due to this effect and the strong alpha-particle absorption, the waves with larger ℓ values experience a smaller fraction of the width of the barrier than do the waves with small ℓ values. This means that the alpha particle is absorbed in some cases before it traverses the entire real part of the optical-model potential, i.e., absorption occurs in the

barrier and the alpha particle does not reach the radius corresponding to the inner turning point of the barrier. Such a model leads to T_{ℓ} values which may be larger than those calculated from models in which it is assumed that the alpha particle is not absorbed in the barrier region.

The reaction cross sections obtained with Eq. (1) for the square-well potential,^(1,2) the optical-model potential, and the parabolic approximation to the real part of the optical model potential are plotted for comparison in Fig. 3 for a $^{23}\text{V}^{51}$ target and in Fig. 4 for a $^{92}\text{U}^{235}$ target. The square-well potential with $r = (1.5A^{1/3} + 1.21)$ fermi gives reaction cross sections which are smaller by a factor of two than the optical-model values. Approximate agreement between the square-well and optical-model cross sections can be obtained for larger values of the square-well radius. If the value of Δ in the square-well radius, $r = r_0 A^{1/3} + \Delta$, is 1.2 fermi, then r_0 must be equal to 1.63 fermi for uranium and 1.9 fermi for vanadium in order to give agreement. Stated in another way, if r_0 in the square-well radius is 1.5 fermi, then Δ must be equal to 2.0 fermi for uranium and 2.7 fermi for vanadium in order that the square-well model gives cross sections as large as the optical model.

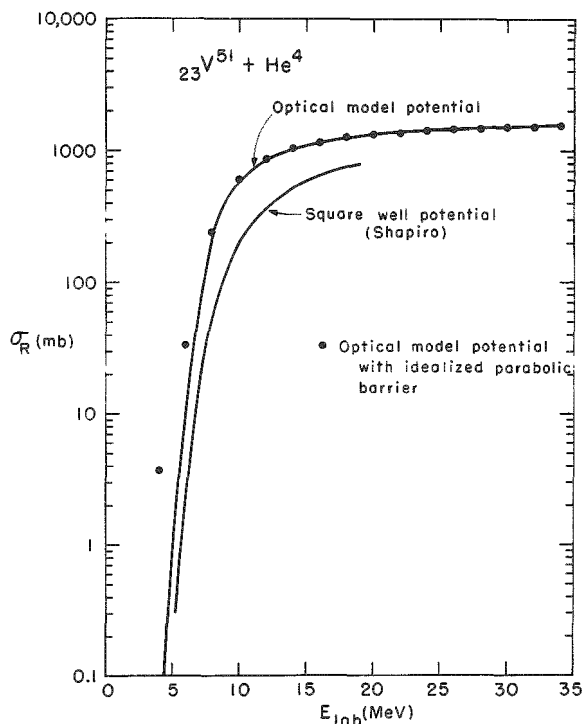


Fig. 3

Reaction cross sections for $^{23}\text{V}^{51} + {}_2\text{He}^4$ are plotted versus the alpha-particle energy in the laboratory system.

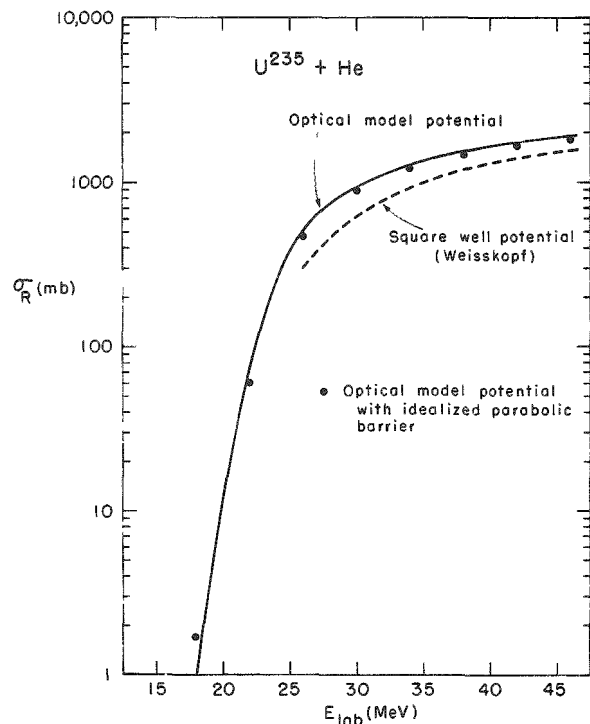


Fig. 4

Reaction cross sections for $^{92}\text{U}^{235} + {}_2\text{He}^4$ are plotted versus the alpha-particle energy in the laboratory system.

A square-well radius of $(1.5A^{1/3} + 2.2)$ fermi will give reaction cross sections which agree reasonably well with optical-model cross sections for a number of elements.

The agreement between the reaction cross sections derived from the optical model and from a model which approximates the real part of the optical-model potential by a parabola and utilizes the transmission coefficients for a parabolic potential is very good for energies exceeding the classical barrier height ($\ell=0$). The degree of agreement in cross sections for vanadium with alpha-particle bombarding energies greater than 8 Mev and for uranium with energies greater than 20 Mev can be seen in Figs. 3 and 4, respectively. At energies below the classical barrier, the agreement between the transmission coefficients and reaction cross sections derived from the two models is unsatisfactory. The merit of the model which utilizes the parabolic approximation of the real part of the optical-model potential lies, of course, in the relatively simple mathematical computation which is necessary for calculating rather accurate reaction cross sections.

The ratios of the reaction cross section for angular momentum ℓ to the total reaction cross section, σ_R^{ℓ}/σ_R , are plotted against ℓ in Fig. 5 for 12-Mev (Lab) alpha particles on $^{23}\text{V}^{51}$ for the three models discussed above. Reasonably good agreement is obtained between the optical- and parabolic-potential models. This results from the fact that the cross sections and the individual transmission coefficients are approximately equal for these two models at all energies greater than the classical barrier.

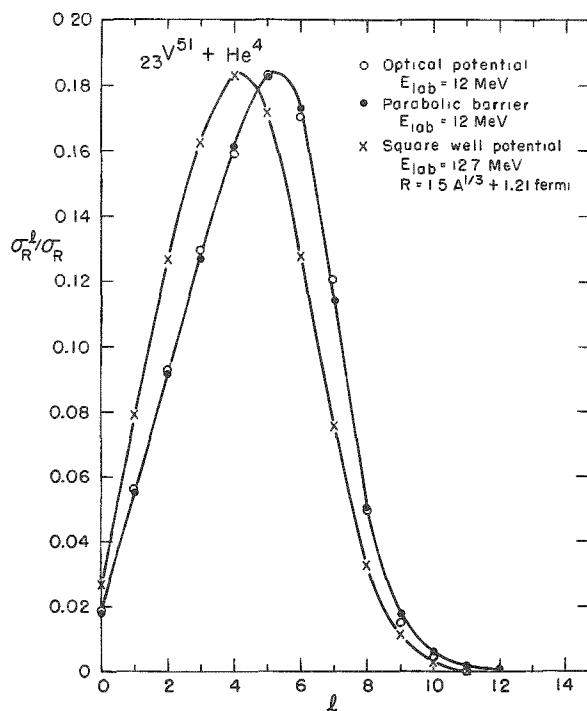


Fig. 5

The ratios of the reaction cross section for angular momentum ℓ to the total reaction cross section, σ_R^{ℓ}/σ_R , are plotted versus ℓ for 12-Mev (Lab) alpha particles on $^{23}\text{V}^{51}$ for the three models discussed in the text.

The square-well model ($r = 1.5A^{1/3} + 1.2$) gives considerably smaller average angular momentum deposited in that the reaction cross sections are less by a factor of two. If the square-well radius is increased to give agreement between the square-well and optical-model cross sections, then the average angular momentum deposited in the square-well model is greater than in the optical model. The square-well model leads to considerable reflection from the spike in the potential barrier and, in order to reproduce the magnitude of the optical-model cross sections, more waves are required in the square-well model.

C. Optical-model Cross-section Dependence on Nuclear Potential

This section is concerned with an investigation of the dependence of the reaction cross section on the nuclear potential in the optical-model calculation.

The first comparison of reaction cross sections in this section are for different sets of Woods-Saxon parameters which give equally good fits to the complex nuclear potential of Eq. (2) for values of r where the real part of the nuclear potential is greater than -10 Mev. The relevant data are summarized in Table IV. The two sets of parameters for uranium (1) $V = -50$ Mev, $W = -27$ Mev, and $r = 8.99$ fermi, and (2) $V = -25$ Mev, $W = -13.9$ Mev and $r = 9.39$ fermi, give approximately the same complex nuclear potential for values of the radius greater than 10 fermi. The reaction cross sections for these two different sets of Woods-Saxon parameters agree very well at both 22 and 38 Mev. Similar cross-section comparisons are made for vanadium. The two sets of Woods-Saxon parameters in Table IV do not give quite as good agreement in the reaction cross-section values for the lighter nucleus, vanadium.

Table IV

REACTION CROSS-SECTION DEPENDENCE ON VARIOUS SETS OF WOODS-SAXON PARAMETERS WHICH GIVE APPROXIMATELY THE SAME COMPLEX NUCLEAR POTENTIALS FOR r VALUES WHERE THE REAL PART OF THE NUCLEAR POTENTIAL IS GREATER THAN -10 MEV.*

Nuclide	E_{Lab} (Mev)	V (Mev)	W (Mev)	r_0 (fermi)	n	σ_R (mb)
$^{23}_{\text{V}}\text{V}^{51}$	6	-50	-10	$1.17A^{1/3} + 1.77$	6.04	10.5
	6	-25	-5.2	$1.17A^{1/3} + 2.17$	6.04	10.6
	34	-50	-10	$1.17A^{1/3} + 1.77$	6.04	1559
	34	-25	-5.2	$1.17A^{1/3} + 2.17$	6.04	1492
	22	-50	-27	$1.17A^{1/3} + 1.77$	10.04	76.8
	22	-25	-13.9	$1.17A^{1/3} + 2.17$	10.04	77.2
	38	-50	-27	$1.17A^{1/3} + 1.77$	10.04	1550
	38	-25	-13.9	$1.17A^{1/3} + 2.17$	10.04	1552

*In all cases

$$d(\text{fermi}) = 0.576$$

and

$$r_c(\text{fermi}) = 1.17A^{1/3}$$

The result of comparisons in Table IV confirms earlier suggestions that the depth of the potential for small r values is unimportant in analyzing alpha-particle elastic scattering and total reaction cross-section data as long as the set of parameters in the Woods-Saxon potential accurately reproduces the complex potential near the nuclear surface.

Whereas the cross-section comparisons in Table IV are for sets of optical-model parameters which give approximately the same complex potential at r values larger than the nuclear radius (although considerably different complex potentials at small values of r), the comparisons in Table V are for sets of optical-model parameters which give different complex nuclear potentials for large values of r .

Table V

REACTION CROSS-SECTION DEPENDENCE ON THE COMPLEX NUCLEAR POTENTIAL*

Nuclide	E_{Lab} (MeV)	V(MeV)	W(MeV)	n	σ_R (mb)
$^{23}_{\Lambda}\text{V}^{51}$	6	- 50	-10	0.04	10.5
	6	0	-10	0.04	3.1
	6	- 50	-10	0.04	11.0
	6	-100	-10	0.04	18.8
	6	- 50	- 2	0.04	6.9
	6	- 50	-11	0.04	10.6
	6	- 50	-20	0.04	12.3
	34	- 50	-10	0.04	1559
	34	0	-10	0.04	1165
	34	- 53	-10	0.04	1571
	34	-100	-10	0.04	1722
	34	- 50	- 2	0.04	1119
	34	- 50	-11	0.04	1560
	34	- 50	-20	0.04	1612
$^{92}_{\Lambda}\text{U}^{235}$	18	- 50	-27	10.04	0.97
	18	- 50	-54	10.04	1.75
	22	- 50	-27	10.04	76.8
	22	0	-27	10.04	43.0
	22	- 53	-27	10.04	79.5
	22	-100	-27	10.04	122.2
	22	- 50	- 4	10.04	48.8
	22	- 50	-30	10.04	80.2
	22	- 50	-54	10.04	104.5
	38	- 50	-27	10.04	1550
	38	0	-27	10.04	1272
	38	- 53	-27	10.04	1562
	38	-100	-27	10.04	1705
	38	- 50	- 4	10.04	1438
	38	- 50	-30	10.04	1560
	38	- 50	-54	10.04	1630

*In all cases

$$r_0(\text{term1}) = 1.17A^{1/3} + 1.77$$

$$d(\text{term1}) = 0.576$$

$$r_c(\text{term1}) = 1.17A^{1/3}$$

The first entry for each energy in Table V gives the appropriate cross section for the Woods-Saxon parameters of Table I, which are based on the experimental nuclear potential⁽⁴⁾

$$-1100 \exp \left[-\left(\frac{r-1.17A^{1/3}}{0.574} \right) \right] - 45.7 i \exp \left[-\left(\frac{r-1.40A^{1/3}}{0.578} \right) \right]$$

for large r values (i.e., values of r where the real part of the potential is greater than -10 Mev). The remainder of the entries for each energy are for various values of the complex nuclear potential. The parameters V and W are varied separately with the other Woods-Saxon parameters fixed such that the change in the complex nuclear potential at large values of r is proportional to the change in V or W. For example, the set of Woods-Saxon parameters for U²³⁵ (V = -100 Mev, W = -27 Mev, r₀ = 1.17A^{1/3} + 1.77, etc.) correspond to a complex nuclear potential equal to

$$-2200 \exp \left[-\left(\frac{r-1.17A^{1/3}}{0.574} \right) \right] - 45.7 i \exp \left[-\left(\frac{r-1.40A^{1/3}}{0.578} \right) \right]$$

for large values of the radius, or a change of a factor of two in the real part of the nuclear potential. Since the uncertainty in the real part of the nuclear potential as determined by analyses⁽⁴⁾ of the elastic-scattering data is thought to be approximately 50%, the above value of the real potential is outside the limit of this error.

The uncertainty in the imaginary part of the nuclear potential as determined by alpha-particle elastic scattering is, however, considerably larger than the uncertainty in the real part of the nuclear potential, and may be as much as 100% or even larger. The set of parameters for U²³⁵ (V = -50 Mev, W = -54 Mev, r₀ = 1.17A^{1/3} + 1.77, etc.) corresponds to a complex nuclear potential equal to

$$-1100 \exp \left[-\left(\frac{r-1.17A^{1/3}}{0.574} \right) \right] - 91.4 i \exp \left[-\left(\frac{r-1.40A^{1/3}}{0.578} \right) \right]$$

at the nuclear surface, which represents a change of a factor of 2 in the imaginary part of the nuclear potential from the average value⁽⁴⁾ deduced from elastic scattering.

At energies considerably larger than the classical barrier, the cross sections vary only slightly with large variations in either the real or imaginary part of the nuclear potential. Variation of either the real or imaginary potential by a factor of 2 at large values of r changes the reaction cross section by only 10% or less. In the region of the Coulomb barrier, however, the reaction cross sections vary considerably with large changes in the complex nuclear potential. The strong dependence of the reaction cross section on the real and imaginary potentials at large values of r for energies near the Coulomb barrier can be seen from the

data of Table V. For the target nucleus U^{235} a change in W from -27 to -54 Mev increases the reaction cross section by 36% for 22-Mev alpha particles and by 80% for 18-Mev alpha particles. Since reaction cross-section values are very sensitive to the complex nuclear potential at energies below the classical barrier, accurate experimental measurements of the reaction cross sections for alpha particles at these energies in conjunction with the alpha-particle elastic-scattering data would be useful in the determination of the complex nuclear potential.

D. Program Checks

The results of our program were checked with data published by Glassgold for 10-Mev protons⁽¹⁰⁾ on argon and copper and for 22-Mev helium ions on silver.⁽¹¹⁾ Some of the other quantities recorded in our program are the Coulomb functions and the real and imaginary parts of the nuclear phase shifts for each ℓ . The authors will supply any of this information to those interested on request.

III. ACKNOWLEDGMENTS

One of the authors (JRH) wishes to thank Professors I. Perlman and J. O. Rasmussen for their hospitality during his summer visit at the Lawrence Radiation Laboratory in Berkeley. We also wish to thank J. O. Rasmussen, R. Griffioen, and R. Vandenbosch for several helpful discussions.

References

1. M. M. Shapiro, Phys. Rev. 90, 171 (1953).
2. J. M. Blatt and V. F. Weisskopf, Theoretical Nuclear Physics (John Wiley and Sons, Inc., New York, 1952), p. 352.
3. H. Feshbach, M. M. Shapiro, and V. F. Weisskopf, NYO-3077, unpublished.
4. G. Igo, Phys. Rev. 115, 1665 (1959).
5. K. W. Ford and D. L. Hill, Phys. Rev. 94, 1617 (1954).
6. R. Hofstadter, Annual Review of Nuclear Science (Annual Reviews, Inc., Palo Alto, California, 1957), Vol. 7, p. 231.
7. R. D. Woods and D. S. Saxon, Phys. Rev. 95, 577 (1954).
8. Suggested by J. O. Rasmussen and programmed by T. D. Thomas, Phys. Rev. 116, 703 (1959).
9. D. L. Hill and J. A. Wheeler, Phys. Rev. 89, 1102 (1953), in particular, p. 1140.
10. A. E. Glassgold, W. B. Cheston, M. L. Stein, S. B. Schuldt, and G. W. Erickson, Phys. Rev. 106, 1207 (1957).
11. W. B. Cheston and A. E. Glassgold, Phys. Rev. 106, 1215 (1957).